Surface and interior anion solvation in water clusters

O Cheshnovsky, R Giniger, G Markovich, G Makov,
A Nitzan, J Jortner

School of Chemistry, Tel Aviv University, Ramat Aviv, 69978 Tel Aviv, Israel

Abstract

We describe the cluster size dependence of the vertical electrostatic stabilization energies $E_{STAB}(n)$ of mass-selected $I^-(H_2O)_n$ ($n = 7$-60) clusters in terms of classical electrostatic solvation models for interior solvation, solvation inside the cluster surface and solvation on the cluster surface. Surface anion solvation in clusters of polar and polarizable molecules yields higher vertical electron detachment energies than those for internal anion solvation. The experimental results for $E_{STAB}(n)$ fit somewhat better the model of anion surface solvation and extrapolate well to a value of $E_{STAB}(\infty)$ for solvation inside the surface.

Resumé

Les énergies verticales de stabilisation electrostatiques $E_{STAB}(n)$ d'agrégats $I^-(H_2O)_n$ ($n = 7$-60) sélectionnés en masse sont discutées à l'aide de modèles classiques de solvatation électrostatique: solvatation au coeur, sous la surface ou à la surface des agrégats. La solvatation d'anions en surface d'agrégats de molécules polaires ou polarisables conduit à des énergies verticales de détachement de l'électron plus grandes que celles obtenues pour des anions solvatés au coeur de ces agrégats. Les mesures expérimentales de $E_{STAB}(n)$ sont en meilleur accord avec le modèle de solvation de l'anion en surface et évoluent vers une solvatation sous le surface de l'agrégat lorsque n tend vers l'infini.

Keywords

Solvation, ion solvation, photoelectron spectroscopy, clusters.

I. Introduction

Clusters provide a fascinating hunting ground for the exploration of the phenomena of microscopic solvation. A central feature of the energetic, thermodynamic, spectroscopic and dynamic cluster size effects [1] for solvation in clusters of polar molecules, pertains to the existence of distinct surface and interior configurations of an anion or a solvated electron on and in clusters (Fig. 1). Surface excess electron states were theoretically predicted [2-6] but not conclusive yet experimentally observed [7, 8] for medium-sized $(H_2O)^-_n$ ($n < 32$) clusters, where surface excess electron localization is due to a large cluster reorganization energy, which cannot be compensated by the electron–cluster interaction for the interior state [2-6]. For large $(H_2O)^-_n$ ($n > 32$) and $(NH_3)^-_n$ ($n > 41$) clusters, the interior excess electron state is expected to be energetically stable [2-6]. Regarding solvated anion clusters [9-16], both molecular dynamic (MD) simulations [17-25] and ab-initio quantum mechanical computations [26-29] indicate that the surface structure dominates for $X^-(H_2O)_n$ clusters ($X = F, C\ell, Br, I$) with a few ($n = 2, 3$) solvent molecules [10-24, 26, 27] and that interior $F^-(H_2O)_n$ ($n = 4, 5$)

structures are stable ([25, 28]). However, the agreement between the conclusions of MD and quantum mechanical calculations ends here. MD simulations ([17-25]) indicate that the surface structure dominates for large $X^-(H_2O)_n$ clusters ($X = C\ell, Br, I$; $n \leq 20$), while quantum mechanical calculations ([25-27, 29]) show that the interior state of $I^-(H_2O)_n$ is realized at $n = 6$ ([29]). The cluster size corresponding to the surface-interior 'transition' is expected to be anion-specific ([19-29]). Recent Monte-Carlo simulations ([30]) for small $C\ell^-(H_2O)_n$ clusters indicate a transition temperature above which interior states become the dominating structures. In view of the intrinsic difficulties in the extension of the quantum mechanical calculations for larger ($n > 8$) clusters and for finite temperatures, and the questionable information emerging from MD simulations, which rest on relatively simple empirical potentials, the distinction between surface vs interior anion solvation in clusters has to rest on a detailed analysis of experimental energetic and spectroscopic data. In this context, the photoelectron spectra (PES) of $C\ell^-(H_2O)_n$ ($n = 1-7$), $Br^-(H_2O)_n$ ($n = 1-17$) and $I^-(H_2O)_n$ ($n = 1-60$) clusters ([13-16]) provides direct information on the vertical ionization potentials and the electrostatic stabilization energies of the anions. Regarding specific cluster size effects, it was concluded ([13]) that in $I^-(H_2O)_6$ the interior structure is realized, in accord with the conclusions of ab-initio calculations ([29]). In this paper we go beyond specific cluster size effects and describe the cluster size dependence of the binding energies for surface and interior structures of large $X^-(H_2O)_n$ clusters in terms of classical electrostatic solvation models. These results will be confronted with the experimental data ([15-16]) for the binding energies of large, mass-selected, $I^-(H_2O)_n$ ($n = 7-60$) clusters.
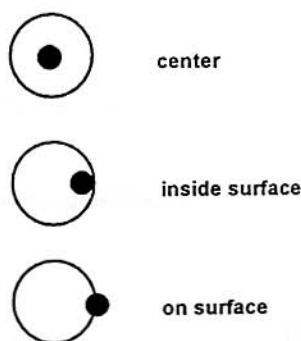

Fig1. Different ion locations (dark circle) used for the classical modeling of the vertical binding energies of anions solvated in clusters.

II. Stabilization Energies of $I^-(H_2O)_n$

The experimental setup is described in detail elsewhere ([13, 16]). The clusters are formed in a pulsed supersonic expansion. Ionization and cluster growth follow the injection of 100-200 eV

electrons from a hot filament source. The clusters are mass-separated by a reflecting time-of-flight mass-spectrometer (a modification of the original linear reflectron ([31])). The mass-selected ions are impulse decelerated to ~ 20 eV kinetic energy, to reduce Doppler-broadening and then are intersected by the electron detaching laser beam. All the PES are taken with 7.1 eV photons (typically 50-150 μjoules), generated by Raman shifting of the 3rd harmonic of a Nd:YAG laser (150 mJ) in 1.2 bar H_2, up to the 7th anti-stokes (AS) line. The spectrometer is calibrated with PES of the bare halogen anions ($C\ell^-, Br^-, I^-$) ([32]). The kinetic energy distribution of the electrons is analyzed with a 250 cm magnetic TOF photoelectron spectrometer ([33]). The photoelectron spectrometer follows the design principles of Kruit and Read ([34]), and is based on a "magnetic bottle" configuration. Its energy resolution is ~ 50 meV at electron kinetic energy of 1.5 eV. We estimate the temperature of the clusters in our experiment to be lower than 100^0 K. This estimate is based on the appearance of the $I^-(H_2O)_n \cdot Ar$ clusters (n = 20) in the mass spectrum and on a spectroscopic analysis of $I^- \cdot CO_2$ (65^0 K) produced under similar source conditions ([35]).

The vertical ionization potentials IP(n) (i.e., the vertical binding energies of the electron to the cluster), were obtained from the peaks of the PES spectra. The vertical stabilization energies $E_{STAB}(n)$ of the anion by the cluster in its equilibrium configuration were obtained from

$$E_{STAB}(n) = IP(n) - EA \ , \tag{1}$$

where EA is the electron affinity of the appropriate bare neutral atom. The experimental $E_{STAB}(n)$ data for $I^-(H_2O)_n$ (n = 1-60) are presented in Fig. 2.

III. Interior Anion Solvation

The electrostatic stabilization energy of an anion solvated in the center of a cluster of radius R can be approximated by the classical continuum dielectric model ([4])

$$E_{STAB}(R) = E_{STAB}(\infty) - (e^2/2R) \ [1-(2/\epsilon_s)+(1/\epsilon_\infty)] \ , \tag{2}$$

where $E_{STAB}(\infty) = IP(\infty)-EA$ is the corresponding bulk value, and ϵ_s and ϵ_∞ are the static and optical dielectric constants of the medium, respectively. In view of our ignorance of the structure and density of water in the $I^-(H_2O)_n$ clusters, which is presumably an amorphous solid at the estimated temperature of T < 100 K (see section II), we shall take the same values of ϵ_∞ for the liquid and the solid, i.e., $\epsilon_\infty = 1.8$. The static dielectric constant is nearly invariant between the liquid and the solid water ([36]) and we shall take $\epsilon_s = 80$ for the cluster.

A rough estimate of the cluster radius R in terms of n is obtained by using the liquid density ρ_W and expressing the spherical cluster volume as the sum of the volumes of the anion of the water molecules:
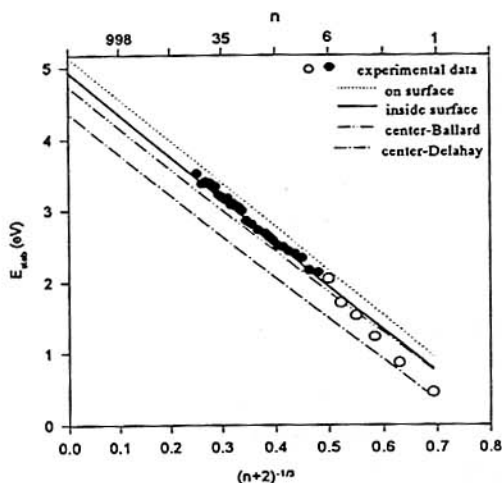
Fig.2: The experimental cluster size dependence of $E_{STAB}(eV)$ for $I^-(H_2O)_n$, o n = 1-6; • n = 7-60, as compared with the theoretical predictions for interior (center), ,inside surface and on-surface solvation. The calculated $E_{STAB}(n)$ values are:

Center-Delahay - from Eqs. (2) and (3) with $E_{STAB}(\infty) = 4.37$ eV (Ref 38); Center-Ballard - from Eqs. (2) and (3) with $E_{STAB}(\infty) = 4.74$ eV (Ref 39); inside surface - from Eqs. (11), (12) and (3) with $E_{STAB}(\infty) = 4.74$ eV; on surface - from Eqs. (17), (19) and (20) with $E_{STAB}(\infty) = 4.74$ eV.

$$4\pi R^3/3 = 4\pi R_{ION}^3/3\eta + 18n/\rho_W N_A \quad , \tag{3}$$

where $R_{ION} = 2.16$Å is the radius of the iodine anion, $\eta = 0.7$ is the volume fraction for the packing of the anion and N_A is Avogadro's number. In view of the uncertainty in the value of η we do not distinguish between packing in the liquid and in the solid. Eq. (3) results in the following expression for $I^-(H_2O)_n$ clusters

$$E_{STAB}(n) = E_{STAB}(\infty) - A(n+\xi)^{-1/3} \quad , \tag{4}$$

where $\xi = 2.0$ represents the self volume of the anion in terms of the water molecule volume. The calculated slope is $A = 5.76$ eV.

The asymptotic value of $E_{STAB}(\infty)$ in Eq. (4) was reported from photoemission studies of I^- in liquid water, which resulted in two experimental values, $E_{STAB}(\infty) = 4.37$ eV obtained by Dalahay [38] from photoemission yields and $E_{STAB}(\infty) = 4.74$ eV extracted from the data of Ballard and coworkers [39] from photoemission yields.

In Fig. 2 we display the experimental values of $E_{STAB}(n)$ vs $(n+2.0)^{-1/3}$, being plotted according to the relation suggested by Eq. (4). The experimental data for n = 7-60 obey well this cluster size equation, with the parameters A = 6.2 eV and $E_{STAB}(\infty)$ = 5.07 eV .

The experimental size dependence of $E_{STAB}(n)$, as manifested by the slope A, appears to agree reasonably well with the prediction of Eq. (4). However, the value of $E_{STAB}(\infty)$ emerging from the cluster size equation is higher (by 0.3-0.7 eV) than the experimental values ([38], [39]) reported for I^- in the bulk water. This discrepancy can arise from one (or both) of the following effects:

(A)   A higher bulk value of $E_{STAB}(\infty)$ in rigid clusters. The $I^-(H_2O)_n$ clusters are characterized by a moderately low temperature (T < 100K, see section II) and are rigid. Accordingly, the bulk value $E_{STAB}(\infty)$ obtained from the analysis of Fig. 2 corresponds to the (amorphous) solid, which differs from the experimental values of $E_{STAB}(\infty)$ in the bulk liquid. The modification of short-range interactions between the cluster and the bulk liquid may result in the increase of $E_{STAB}(\infty)$ in the solid.

(B)   The enhancement of $E_{STAB}(\infty)$ due to surface anion solvation. We shall advance in sections IV and V the surprising result that $E_{STAB}(\infty)$ is higher for surface solvation than for bulk solvation. Accordingly, anion surface solvation (in the range n < 60) may be responsible for the high value of $E_{STAB}(\infty)$ obtained from Fig. 2.

We shall now examine two models for surface solvation, that involving inside surface solvation and where the anion constitutes a part of the surface.

V. Anion Solvation Inside the Cluster Surface

A relatively high degree of surface solvation corresponds to the "dipping" of the anion just below the surface of the cluster (Fig. 1).   To calculate the vertical electrostatic stabilization energy $E_{STAB}(r, R)$ for the anion in the cluster, we have utilized the electrostatic model ([40]) of Brus ([41]) for the electrostatic potential induced at the distance r (where $r \leq R-R_{ION}$) from the cluster center by an ion of charge -e and radius R_{ION}, which is located within a sphere of radius R and static and optical dielectric constants ϵ_s and ϵ_∞. The vertical stabilization energy is

$$E_{STAB}(r, R) = -W(r, R, \epsilon_\infty) + e[\phi(r, R, \epsilon_\infty) - \phi(r, R, \epsilon_s)] , \qquad (5)$$

where $W(r, R, \epsilon_\infty)$ is the charging energy of the ion in a medium with a dielectric constant ϵ_∞,

$$W(r, R, \epsilon_\infty) = (e^2/2R_{ION})[(1/\epsilon_\infty)-1] + (e^2/2R) \sum_{j=0}^{\infty} f_j(\epsilon_\infty)(r/R)^{2j} \qquad (6)$$

and $\phi(r, R, \epsilon)$ is the potential induced at r in a dielectric sphere of a dielectric constant ϵ,

$$\phi(r, R, \in) = (e/\in R_{ION}) + (e/R) \sum_{j=0}^{\infty} f_j(\in)(r/R)^{2j} \ . \tag{7}$$

The second term of the RHS of Eq. (6) constitutes the potential due to the 'permanent' dipolar dielectric polarization. The auxiliary functions $f_j(\in)$ in Eqs. (7) and (8) are given by

$$f_j(\in) = (\in -1)(j+1)/\in(j\in +j+1) \tag{8}$$

Eqs. (6)-(9) result in the final expression for the vertical stabilization energy

$$E_{STAB}(r, R) = (e^2/2R_{ION})(1-2/\in_s +1/\in_\infty) +$$
$$+ (e^2/2R) \sum_{j=0}^{\infty} [f_j(\in_\infty)-2f_j(\in_s)](r/R)^{2j} \ , \tag{9}$$

The first term on the RHS of Eq. (9) can be identified with the bulk value

$$E_{STAB}(\infty) = \frac{e^2}{2R_{ION}} \left[1 - \frac{2}{\in_s} + \frac{1}{\in_\infty} \right] \ . \tag{10}$$

Eq. (9) can now be recast in the alternative form

$$E_{STAB}(r, R) = E_{STAB}(\infty) - (e^2/2R)(1+1/\in_\infty -2/\in_s) +$$
$$+ (e^2/2R) \sum_{j=1}^{\infty} [f_j(\in_\infty)-2f_j(\in_s)](r/R)^{2j} \ , \tag{11}$$

where the third term at the RHS of Eq. (11) constitutes the surface correction to the interior stabilization energy, Eq. (2). We shall now consider the inside surface vertical stabilization energy by setting $r = R-R_{ION}$ in Eq. (11), i.e.,

$$E_{STAB}^{IS}(R) = E_{STAB}(R-R_{ION}, R) \ . \tag{12}$$

In the bulk limit ($R \to \infty$), Eq. (11) will result in $E_{STAB}^{IS}(\infty)$ for the 'dipping' of the anion just below the macrosurface. The second term and the low j terms in the third term on the RHS of Eq. (11) vanish. The sum on the RHS of Eq. (11) with sufficiently large values of j is represented in terms of a geometric series with $f_j(\in)$ being independent of j. Eq. (11) then results in

$$E_{STAB}^{IS}(\infty) = E_{STAB}(\infty) + \left[\frac{e^2}{4R_{ION}}\right] \left[\frac{(\epsilon_\infty-1)}{\epsilon_\infty(\epsilon_\infty+1)} - 2\frac{(\epsilon_s-1)}{\epsilon_s(\epsilon_s+1)}\right] . \tag{13}$$

As is apparent from Eq. (13), in the limit used by Bruce [41] when $\epsilon_\infty = \epsilon_s$, $E_{STAB}^{IS}(\infty) < E_{STAB}(\infty)$, while for clusters of polar molecules, where $\epsilon_\infty \ll \epsilon_s$, we obtain $E_{STAB}^{IS}(\infty) > E_{STAB}(\infty)$, revealing the increase of the electrostatic binding energy relative to the bulk value for interior surface solvation. For the $I^-(H_2O)_n$ system, this increase amounts to $E_{STAB}^{IS}(\infty)-E_{STAB}(\infty) = 0.22$ eV.

The cluster size dependence of the calculated $E_{STAB}^{IS}(n)$, Eqs. (11), (12) and (3), is portrayed in Fig. 2. The results of this model are quite close to the experimental data (Fig. 2), provided that $E_{STAB}(\infty)$ is represented by the experimental bulk value of Ballard et al. [39], and Eq. (13) is used to calculate the correction term for $E_{STAB}^{IS}(\infty)$. The interesting trend of the increase of the asymptotic value of $E_{STAB}(\infty)$ for surface solvation, which is manifested for inside surface solvation on a macrosurface, is further enhanced for on-surface solvation, which we now consider.

V. Anion Solvation on the Cluster Surface

When the ion is too close to the cluster surface, i.e., $R \geq R-R_{ION}$, the starting point for the calculation in Section IV, Eq. (6), ceases to be valid. Makov and Nitzan [42] have recently developed the necessary modification which makes it possible to study ions at such close vicinity to the cluster surface, and in particular the vertical detachment of an electron from a negative ion solvated at the surface of a dielectric sphere (Fig. 1).

Consider first an ion positioned on the planar boundary between two dielectric media 1 and 2. The generalization of the Born expression for the solvation free energy of this case yields [40]

$$\Delta E_s = -\left[\frac{\epsilon_{s1}+\epsilon_{s2}-2}{\epsilon_{s1}+\epsilon_{s2}}\right]\left[\frac{e^2}{2R_{ION}}\right] , \tag{14}$$

where ϵ_{si} (i = 1,2) is the static dielectric response of medium i. We note in passing that for $\epsilon_{s1} = \epsilon_{s2} = \epsilon_s$ the usual Born expression, $\Delta E = -(1-\frac{1}{\epsilon_s})e^2/2R_{ION}$, is obtained. The vertical solvation energy ΔE_s^v is given by an expression analogous to (14) in which $\epsilon_{\infty1}$ and $\epsilon_{\infty2}$ replace ϵ_{s1} and ϵ_{s2}, respectively. The stabilization energy is given by [40]

$$E_{STAB} = \Delta E_s^v - 2\Delta E_s . \tag{15}$$

If the Born expression for solvation in bulk dielectric is used for ΔE_s^v and ΔE_s in Eq. (15), we obtain Eq. (10) for $E_{STAB}(\infty)$, while for an ion on the planar interface between two dielectrics we get from (14)

$$E_{STAB}^{OS}(\infty) = \left(\frac{e^2}{2R_{ION}}\right)\left[1 - \left(\frac{4}{\epsilon_s+1}\right) + \left(\frac{2}{\epsilon_\infty+1}\right)\right] , \tag{16}$$

where we have specified to the case $\epsilon_{s1} = \epsilon_s$, $\epsilon_{\infty 1} = \epsilon_\infty$, $\epsilon_{s2} = \epsilon_{\infty 2} = 1$. From Eqs. (10) and (16) follows

$$E_{STAB}^{OS}(\infty) = E_{STAB}(\infty) + \left[\frac{(\epsilon_\infty-1)}{\epsilon_\infty(\epsilon_\infty+1)} - 2\frac{(\epsilon_s-1)}{\epsilon_s(\epsilon_s+1)}\right]\left[\frac{e^2}{2R_{ION}}\right] , \tag{17}$$

The difference between the stabilization energies $E_{STAB}^{OS}(\infty)-E_{STAB}(\infty)$ is negative for $\epsilon_s = \epsilon_\infty$. On the other hand, this difference remains positive for $\epsilon_s \gg \epsilon_\infty > 1$, a situation common for polar solvents. Note that the correction term for on-surface solvation is just twice the correction for solvation inside a macrosurface, Eq. (13).

Next consider the case of a spherical cluster of radius R. Eq. (15) may again be used with the appropriate expressions for ΔE_s and ΔE_s^v in the cluster. For an ion in the center of the cluster ($r = 0$) and on the surface ($r = R$) the following results are obtained [42]:

$$\Delta E_s(r=0) = -\frac{e^2}{2}\left(1 - \frac{1}{\epsilon_s}\right)\left(\frac{1}{R_{ION}} - \frac{1}{R}\right) \tag{18a}$$

and

$$\Delta E_s(r=R) = -\left(\frac{e^2}{2}\right)\frac{(\epsilon_s-1)}{(\epsilon_s+1)}\left[\frac{1}{R_{ION}} - \frac{1}{R}\right] + \frac{(\epsilon_s-1)}{((\epsilon_s+1)^2)}\left(\frac{e^2}{2R}\right)\left[\frac{1}{2} - \ell n\frac{R_{ION}}{R}\right]. \tag{18b}$$

Again $\Delta E_s^v(r=0)$ and $\Delta E_s^v(r=R)$ are obtained from Eqs. (18a) and (18b), respectively, by replacing ϵ_s by ϵ_∞. Eqs. (10) and (18) lead to Eq. (2) for $E_{STAB}(R)$, while for the 'on surface' anion state the size-dependent stabilization energy is

$$E_{STAB}^{OS}(R) = E_{STAB}^{OS}(\infty) - \left(\frac{e^2}{2R}\right)[\left(1 - \frac{4}{\epsilon_s+1} + \frac{2}{\epsilon_\infty+1}\right)$$
$$- \left(\frac{1}{2} - \ell n\left(\frac{R_{ION}}{R}\right)\right)\left(\frac{(\epsilon_\infty-1)}{(\epsilon_\infty+1)^2} - \frac{2(\epsilon_s-1)}{(\epsilon_s+1)^2}\right)] , \tag{19}$$

where $E_{STAB}^{OS}(\infty)$ is given by Eqs. (17) and (10). The stabilization energy for the 'on surface' anion (at the cluster vacuum interface) as a function of the number of solvent molecules is given by

$$E_{STAB}^{OS}(n) = E_{STAB}^{OS}(\infty) - (6.14-0.095\ell n(2.0+n))(2.0+n)^{-1/3} . \tag{20}$$

Naturally, there is no experimental value for $E^{OS}_{STAB}(\infty)$, thus we have only a crude estimate of the asymptotic value of Eq. (20). We find that $E^{OS}_{STAB}(\infty) - E_{STAB}(\infty) = 0.44$ eV, revealing an increase of $E^{OS}_{STAB}(\infty)$ relative to $E_{STAB}(\infty)$, Eq. (10), for the centrally solvated anion. As is apparent from Fig. 2, the on surface stabilization (with the Ballard et al. value [39] $E_{STAB}(\infty) = 4.74$ eV), consistently overestimates the experimental results.

VI. Concluding Remarks

The surprising result emerging from our analysis is that surface anion solvation in clusters of polar molecules yields higher vertical electron detachment energies than internal solvation. This conclusion is valid, within the framework of the simple dielectric model, both for the on surface and for the inside surface solvation, as compared to the interior central solvation. The comparison between the central, inside surface and on surface vertical stabilization energies reveals that the increase in $E_{STAB}(\infty)$ and in $E_{STAB}(n)$ (for a fixed n) on going from the cluster center to the cluster surface is monotonous. The interesting features of the continuum model, $E_{STAB}(n) < E^{IS}_{STAB}(n) < E^{OS}_{STAB}(n)$ for sufficiently large n in clusters of polar solvents, is qualitatively different from the results of quantum mechanical computations [27, 29] for small $I^-(H_2O)_n$ (n = 2-8) clusters, which yield larger values of $E_{STAB}(n)$ for interior solvation than for surface solvation.

It will be instructive to consider the range of ϵ_∞ and ϵ_s for which the surface vertical stabilization energy exceeds the corresponding interior value, i.e., $\delta^{IS} = E^{IS}_{STAB}(\infty) - E_{STAB}(\infty) > 0$ and $\delta^{OS} = E^{OS}_{STAB}(\infty) - E_{STAB}(\infty) > 0$. This analysis will also provide an insight into the nature of the surface solvation enhancement of the vertical stabilization energy. To elucidate the general physical treatment we shall limit ourselves to the exploration of the energetics in the bulk and macrosurface limit. The vertical stabilization energies, Eqs. (10), (13), and (17) for interior bulk and for macrosurfaces can be expressed as sums of (negative) heats of solution (ΔE_S) and medium organization energies in the absence of the anion (χ), i.e., $E_{STAB}(\infty) = \Delta E^B_S + \chi^B$, $E^{IS}_{STAB}(\infty) = \Delta E^{IS}_S + \chi^{IS}$ and $E^{OS}_{STAB}(\infty) = \Delta E^{OS}_S + \chi^{OS}$, with the individual contributions

$$\Delta E^B_S = (e^2/2R_{ION})(1-1/\epsilon_s) \tag{21a}$$

$$\Delta E^{IS}_S = \Delta E^B_S - (e^2/4R_{ION})[(\epsilon_s-1)/\epsilon_s(\epsilon_s+1)] \tag{21b}$$

$$\Delta E^{OS}_S = \Delta E^B_S - (e^2/2R_{ION})[(\epsilon_s-1)/\epsilon_s(\epsilon_s+1)] \tag{21c}$$

and

$$\chi^B = (e^2/2R_{ION})[(1/\epsilon_\infty)-(1/\epsilon_s)] \tag{22a}$$

$$\chi^{IS} = \chi^B + (e^2/4R_{ION})\left[\frac{(\epsilon_\infty-1)}{\epsilon_\infty(\epsilon_\infty+1)} - \frac{(\epsilon_s-1)}{\epsilon_s(\epsilon_s+1)}\right] \tag{22b}$$

$$\chi^{OS} = \chi^B + (e^2/2R_{ION})\left[\frac{(\epsilon_\infty-1)}{\epsilon_\infty(\epsilon_\infty+1)} - \frac{(\epsilon_s-1)}{\epsilon_s(\epsilon_s+1)}\right], \tag{22c}$$

where the superscripts B, IS and OS refer to the bulk, inside surface and on surface, respectively. From these results one can immediately infer the reduction of the heat of solvation for the surface solvation relative to the interior solvation for all situations, i.e., $\Delta E_s^{IS} - \Delta E_s^B < 0$ and $\Delta E_s^{OS} - \Delta E_s^B < 0$ for all values of ϵ_s and ϵ_∞. The behavior of χ is more interesting and diverse, and three cases will be considered:

(1) A nonpolar medium, i.e., $\epsilon_s = \epsilon_\infty$. All the medium reorganization energies vanish, i.e., $\chi = \chi^{IS} = \chi^{OS} = 0$, whereupon $\delta^{IS} < 0$ and $\delta^{OS} < 0$. Thus, in a nonpolar medium the vertical stabilization energy, which is equal to the heat of solution, is reduced at the surface.

(2) A nonpolarizable polar medium. To explore the effect of the orientation of the permanent dipoles, we shall consider a hypothetical medium with $\epsilon_\infty = 1$ and $\epsilon_s > 1$. For such a medium $\chi^{IS} - \chi^B < 0$ and $\chi^{OS} - \chi^B < 0$, so that the medium reorganization energy due to permanent dipole-permanent dipole interaction is reduced at the surface. Accordingly, $\delta^{IS} < 0$ and $\delta^{OS} < 0$, exhibiting the reduction of the vertical stabilization energies upon surface solvation.

(3) A polar polarizable medium with $\epsilon_\infty > 1$ and $\epsilon_s \gg 1$. For such a medium $\chi^{IS} - \chi^B > 0$ and $\chi^{OS} - \chi^B > 0$. When the increase of the medium reorganization energy dominates the decrease of the heat of solvation we have $\delta^{IS} > 0$ and $\delta^{OS} > 0$, resulting in the increase of the stabilization energy at the surface relative to the interior.

Thus both for a nonpolar medium (case (1)) and for a nonpolarizable polar medium (case (2)) surface reduction of the vertical stabilization energy occurs. The surface enhancement of the vertical stabilization energy is exhibited only for case (3). This interesting new result is not due to the orientation of permanent dipoles, case (2), but rather is traced to the surface enhancement of the repulsive interactions involving induced dipoles, which originate from permanent-dipole-polarizability interactions. The induced dipole - permanent dipole repulsive interaction can be larger for surface solvation, where the surface permanent dipoles are unbalanced, than for the bulk, where the permanent dipoles are oriented around the anion site. Accordingly, for macrosurfaces (and clusters) of polarizable and polar molecules (with large ϵ_s) the induced dipole - permanent dipole repulsions are enhanced on the surface, providing a rationalization for our new results, i.e., $\delta^{IS} > 0$ and $\delta^{OS} > 0$.

We note, however, that conclusions regarding the validity of our simple continuum model for anion solvation in a cluster containing a few tens of polar molecules should be taken with extreme care:

1. The applicability of the simple continuum dielectric model for ion solvation in moderately small (n = 7-60) clusters is questionable. The more sophisticated approach of Rips and Jortner [43], which rests on the mean spherical approximation (MSA), indicates that the continuum model is strictly applicable for n > 125. We shall return later to this issue.

2. The slope obtained from Eqs. (4), (12) and (20) depends on ionic volume, on the water density, and also on ϵ_s and ϵ_∞, which are sensitive to the phase and temperature of water.

3. Although the slope of the plots fits well the classical model, the exact value of $E_{STAB}(\infty)$, $E_{STAB}^{IS}(\infty)$, or $E_{STAB}^{OS}(\infty)$ are uncertain. We believe that the "true" value of $E_{STAB}(\infty)$ should lie between the measured bulk electron emission threshold [38] (4.37 eV) and the peak of the PES of I^- in solution [39] (4.74 eV). This peak, representing the vertical transition in the bulk, is shifted to a

binding energy that is apparently higher than the value of vertical transition in the bulk, due to electron inelastic scattering. We conclude that $E_{STAB}(\infty)$ should lie somewhere below 4.74 eV with a lower bound of 4.37 eV. Our experimental results extrapolate better to the upshifted values for $E_{STAB}^{IS}(\infty)$.

A more sophisticated model, which can be applied to large clusters, rests on the MSA used by Rips and Jortner [43]. This model introduces structure into the electrostatic model. The ion, a hard charged sphere, is solvated in the center of a cluster, consisting of dipole hard sphere solvent molecules with a radial distribution function identical to water at room temperature. The results of this MSA model suffer from strong oscillations in the function of E_{STAB} vs. $n^{-1/3}$, with local minima and plateaus appearing for cluster with n = 12 to 50. In reality, water-water structure is highly dependent on hydrogen bonding, and such local minima are not observed in the experiment. The MSA converges to the continuous dielectric model for clusters with more than 125 water molecules. In spite of its higher sophistication, this model does not seem to have any advantage over the simple continuous dielectric model, and in its current form does not treat the effects of surface solvation.

Acknowledgments

Bibliography

(1) Jortner, J., Z. Phys. D., 24, 247 (1992).
(2) Barnett, R.N., Landman, U., Cleveland, C.L., and Jortner, J., Phys. Rev. Lett., 59, 811 (1987).
(3) Barnett, R.N., Landman, U., Cleveland, C.L., and Jortner, J., J. Chem. Phys., 88, 4421, 4429 (1988).
(4) Barnett, R.N., Landman, U., and Jortner, J., Chem. Phys. Lett., 145, 382 (1988).
(5) Barnett, R.N., Landman, U., Kestner, N.R., and Jortner, J., J. Chem. Phys., 88, 6670 (1988).
(6) Barnett, R.N., Landman, U., and Nitzan, A., J. Chem. Phys., 89, 2242 (1988).
(7) Coe, J.V., Lee, G.H., Eaton, J.G., Arnold, S.T., Sarkas, H.W., Bowen, K.H., Ludewigt, C., Haberland, H., and Worsnop, D.G., J. Chem. Phys., 92, 3980 (1990).
(8) Lee, G.H., Arnold, S.T., Eaton, J.G., Sarkas, H.W., Bowen, K.H., Ludewigt, C., and Haberland, H., Z. Phys. D, 20, 9 (1991).
(9) Lebarle, P., Ann. Rev. Phys. Chem., 28, 445 (1977).
(10) Yang, X., and Castleman, A.W., Jr., J. Phys. Chem., 94, 8599 (1990); 95, 6182 (1991).
(11) Yang, X., Zhang, X., and Castleman, A.W., Jr., J. Phys. Chem, 95, 8520 (1991).
(12) Hiraoka, K., Misuze, S., and Yanabe, S., J. Phys. Chem., 92, 3943 (1988).
(13) Markovich, G., Giniger, R., Levin, M., and Cheshnovsky, J., J. Chem. Phys., 95, 9416 (1991).
(14) Markovich, G., Giniger, R., Levin, M., and Cheshnovsky, O., Z. Phys. D., 20, 69 (1991).
(15) Markovich, G., Pollack, S., Giniger, R., and Cheshovsky, O., Z. Phys. D., 26, 98 (1993).
(16) Markovich, G., Giniger, R., and Cheshnovsky, O., J. Chem. Phys. (in press).
(17) Perera, L., and Berkowitz, M., J. Chem. Phys., 95, 1954 (1991).
(18) Perera, L., and Berkowitz, M., J. Chem. Phys., 99, 4222 (1993).
(19) Dang, L.X., and Garret, B.C., J. Chem. Phys., 99, 2972 (1993).
(20) Caldwell, J., Dang, L.X., and Kollman, P.A., J. Am. Chem. Soc., 112, 9144 (1990).
(21) Dang, L.X., Rice, J.E., Caldwell, J., and Kollman, P.A., J. Am. Chem. Soc., 113, 2481 (1991).
(22) Caldwell, J., Dang, L.X., and Kollman, P.A., J. Am. Chem. Soc., 112, 9145 (1990).
(23) Sung, S. and Jordan, P.C., J. Chem. Phys., 85, 4045 (1986).
(24) Dang, L.X., and Smith, D.E., J. Chem. Phys., 99, 6950 (1993).

(25) Perera, L and Berkowitz, M.L., J. Chem. Phys. (in press).
(26) Combariza, J.E., Kestner, N.R., and Jortner, J., Chem. Phys. Letters, 203, 423 (1993).
(27) Combariza, J.E., Kestner, N.R., and Jortner, J., J. Chem. Phys., 100, 2851 (1994).
(28) Combariza, J.E. and Kestner, N.R., J. Phys. Chem., 98, 3513 (1994).
(29) Combariza, J.E., Kestner, N.R., and Jortner, J., Chem. Phys. Lett., 221, 156 (1994).
(30) Arada, T., Nishimoto, K., and Kitaura, K., J. Phys. Chem., 97, 7724 (1993).
(31) Mamyrin, B.A. and Shmikk, D.V., Sov. Phys. JETP, 49, 762 (1979).
(32) Hotop, H. and Lineberger, W.C., J. Phys. Chem. Ref. Data, 4, 539 (1975).
(33) Cheshnovsky, O., Yang, S.H., Pettiette, C.L., Craycraft, J.J., and Smalley, R.E., Ref. Sci. Instru., 58, 2131 (1987).
(34) Kruit, P. and Read, F.H., J. Phys. E. (Sci. Instrum.), 16, 313 (1983).
(35) Zhao, Y., Arnold, C.C., and Neumark, D.M., J. Chem. Soc. Faraday Trans., 89, 1449 (1993).
(36) Debye, P., Polar Molecules. Dover Publications, Inc., 1929.
(37) Barnett, R.N., Landman, U., Cleveland, C.L., and Jortner, J., Chem. Phys. Letters, 145, 382 (1988).
(38) Delahay, P., Acc. Chem. Res., 15, 40 (1982).
(39) Ballard, R.E., Jones, J., Read, D., Inchley, A., and Cranmer, M., Chem. Phys. Letters, 134, 177 (1987).
(40) Böttcher, C.J.F., The Theory of Electric Polarization. 2nd Ed. Elsevier: Amsterdam, 1973.
(41) Brus, L.E., J. Chem. Phys., 79, 5566 (1983).
(42) Makov, G. and Nitzan, A., J. Phys. Chem., 98, 3459 (1994).
(43) Rips, I. and Jortner, J., J. Chem. Phys., 97, 536 (1992).